ISSN: 1813-4890

A research paper was conducted on the intricate and dynamic lateral vibrations of BHA

Jiang Chao

SINOPEC Southwest Oil & Gas Company, Chengdu 610041, China;

lianjie5189@126.com

Abstract

The Bottom Hole Assembly (BHA) is an important part of oil and gas exploration and development. It affects rock-breaking efficiency, drilling performance, drilling safety, and wellbore trajectory. When drilling in deviated or horizontal well sections, the drilling string is at a higher risk. This is due to the combined effects of drilling pressure and gravity, which cause the BHA to bend laterally below the neutral point, making it prone to significant deformation. When the drilling string is bent, it can cause reverse whirl which leads to more contact with the wellbore wall and causes increased wear. This is especially problematic in deep wells where the bottom rocks are harder and more abrasive and the drill string has lower torsional stiffness. As a result, non-periodic torsional and axial vibrations can occur in the BHA, which can cause the drill string body, connections, and drill bit to fail. To prevent this, a dynamic model for the drilling string below the neutral point must be established and the vibration characteristics of the drill string and BHA analyzed to improve durability, stability, and safety. For the Pengzhou Maritime project 5-2D well, differential equations for the drill string motion were derived using the lumped parameter method, rotor dynamics theory, and the Lagrangian energy method. The drill string and BHA's vibration characteristics, and their correlation with drilling pressure, inclination angle, top drive speed, and drill bit type, were uncovered using numerical methods.

Keywords

BHA, Drill string, Vibrations, Dynamic, Whirl.

1. Introduction

When conducting underground drilling operations, the Bottom Hole Assembly (BHA) can experience lateral vibrations. These vibrations can cause damage to the drill strings, increase the risk of downhole accidents, and reduce drilling efficiency and safety [1-5]. As a result, it is essential to conduct thorough research on the lateral vibration behavior of the BHA to improve the quality and safety of drilling operations.

The lateral vibration of the bottom hole assembly (BHA) is caused by the bending and sliding of the drill string along the wellbore wall, which can have a detrimental impact on the drilling process in two distinct ways. Firstly, it causes stress and deformation in the drill string, making it more vulnerable to wear and corrosion. Secondly, it can result in energy losses and instability in the wellbore due to the friction between the drill string and the wellbore wall. These issues can lead to reduced drilling efficiency, accidents, and work stoppages. Extensive research has been conducted on lateral vibration, which has revealed that several factors, such as drill pressure, top drive speed, drill string stiffness, and wellbore curvature, can affect it. Drill pressure, in particular, is a crucial control factor that can alter the degree of drill string bending and sliding. Furthermore, increases in top drive speed can raise the amplitude and frequency of the vibrations, thereby further impacting the drilling process. Building upon the existing

ISSN: 1813-4890

research, this study aims to further explore the lateral vibration behavior and dynamic mechanisms of the BHA. By employing a combination of experimental and numerical simulation methods, the study will systematically investigate the drilling vibration characteristics under different operating conditions and analyze the influences of drill pressure and top drive speed on lateral vibration. Through a comprehensive understanding of the mechanisms and patterns of lateral vibration, this research aims to provide guidance and recommendations for drilling engineers to better control and mitigate lateral vibrations of the BHA, thereby enhancing drilling efficiency and safety [6-8].

The objective of this study is to conduct a comprehensive analysis of lateral vibration in drilling engineering and propose efficient control approaches and optimization strategies. By examining the lateral vibration characteristics of the Bottom Hole Assembly (BHA), our aim is to present practical solutions for addressing vibration-related issues in drilling operations, thereby improving their safety and efficiency.

2. The dynamic model of the Bottom Hole Assembly (BHA)

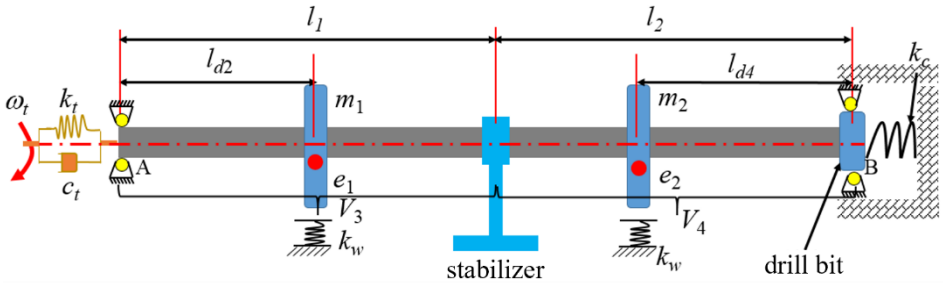

Fig. 1 Dynamic model of the drill string system

As shown in Fig. 1, to analyze the longitudinal-transverse-torsional coupled vibration mechanism of the PZ5-2D wellbore BHA, parameters such as top drive input, drill string-wellbore interaction, drill bit-bottom hole interaction, stabilizers, and drill string eccentricity are taken into account. The motion differential equations of the drill string vibration system below the neutral point are established to study the vibration characteristics of the drill string and BHA below the neutral point. The drill string and BHA below the neutral point are simplified as eccentric rotors with eccentricities e_1 and e_2 and masses m_1 and m_2 respectively, arranged on the circular cross-section of the massless elastic shaft of the drill string and connected through spring dampers. Points A and B represent the neutral point of the drill string and the position of the drill bit respectively. Due to the zero axial force at the neutral point of the drill string and the very small gap between the drill bit and the wellbore, the transverse vibration of the drill string at the positions of the drill bit and the neutral point can be neglected. Therefore, it is assumed that the transverse displacements of the neutral point of the drill string and the position of the drill bit are zero. At the same time, the transverse and axial vibrations of the drill string above the neutral point are neglected, and the drill string above the neutral point in the torsional direction is simulated as a spring-damper with stiffness k_t and damping c_t. Compared to the drill string below the neutral point, the BHA has a higher torsional stiffness, so the torsional deformation of the BHA is neglected.

Assuming that the wellbore center is the coordinate origin for the transverse vibration system of the drill string, the coordinates of the center of mass for the drill string and BHA, denoted as G_1 and G_2 respectively, can be expressed as follows:

$$\begin{cases} G_1 = \left(x_1 + e_1\cos\phi_1, y_1 + e_1\sin\phi_1\right) \\ G_2 = \left(x_2 + e\cos\phi_2, y_2 + e\sin\phi_2\right) \end{cases} \tag{1}$$

ISSN: 1813-4890

Where x_1 and y_1 represent the transverse displacements of the drill string below the neutral point, while x_2 and y_2 represent the transverse displacements of the BHA. ϕ_1 and ϕ_2 denote the rotational angles of the drill string below the neutral point and the BHA, respectively.

The total kinetic energy T of the drill string system below the neutral point is given by:

$$T=\frac{1}{2}m_1G_1\dot{G}_1+\frac{1}{2}m_2G_2\dot{G}_2+\frac{1}{2}J_1\dot{\phi}_1^2+\frac{1}{2}J_2\dot{\phi}_2^2+\frac{1}{2}m_1\dot{z}_1^2+\frac{1}{2}m_2\dot{z}_2^2 \tag{2}$$

Where J_1 and J_2 represent the equivalent moments of inertia of the drill string and BHA, respectively. $\dot{\phi}_1$ and $\dot{\phi}_2$ denote the rotational velocities of the drill string and BHA, while $\dot{z}_1$ and $\dot{z}_2$ represent the axial vibration velocities of the drill string and BHA, respectively.

Analyzing the energy conversion process of the entire system, it is found that in the inclined wellbore section, the gravitational potential energy V_1 of the drill string and the strain potential energy V_2 of the drill string are given by:

$$V_1=m_1\mathrm{g}\cos\alpha\left(x_1-e_1\sin\phi_1\right)-m_1\,\mathrm{g}\sin\alpha z_1+m_2\mathrm{g}\cos\alpha\left(x_2-e_2\sin\phi_2\right)-m_2\,\mathrm{g}\sin\alpha z_2 \tag{3}$$

$$V_2=\frac{1}{2}k_{t1}\left(\phi_1-\phi_2\right)^2+\frac{1}{2}k_t\left(\phi_t-\phi_1\right)^2+k_z\left(z_1-z_2\right)^2 \tag{4}$$

Where g represents the acceleration due to gravity, α denotes the inclination angle of the wellbore, k_{t1} is the equivalent torsional stiffness of the drill string, k_z is the equivalent axial stiffness of the drill string, and ϕ_t, ϕ_1, and ϕ_2 represent the rotation angles of the top drive, drill string, and BHA, respectively.

According to previous studies, the transverse bending strain potential energy of the drill string system is related to the interaction force between the stabilizer and the wellbore wall. Therefore, it is necessary to determine the total transverse bending strain potential energy of the drill string system based on the contact conditions between the stabilizer and the wellbore wall. When there is no contact between the stabilizer and the wellbore wall, the transverse bending strain potential energy of the drill string below the neutral point is determined by the transverse displacements of the drill string and stabilizer together, while the transverse bending strain potential energy of the BHA is determined by the transverse displacements at the drill bit and stabilizer. When contact occurs between the stabilizer and the wellbore wall, due to the frictional forces between them, the center of mass of the drill string and BHA will be offset under the action of the restoring forces generated by elastic deformation, as shown in Fig. 2, the stabilizer-wellbore contact model. The restoring forces generated by elastic deformation can be decomposed into normal support force and tangential force. Because the transverse bending strain potential energy of the drill string system when the stabilizer and the wellbore wall are in contact exists in the form of forces [9]. Furthermore, let the wellbore wall above the wellbore be the positive direction for the transverse vibration of the drill string in the x direction below the neutral point, the positive direction for axial vibration points towards the bottom of the well, and the positive direction for transverse vibration in the y direction is determined by the right-hand rule.

ISSN: 1813-4890

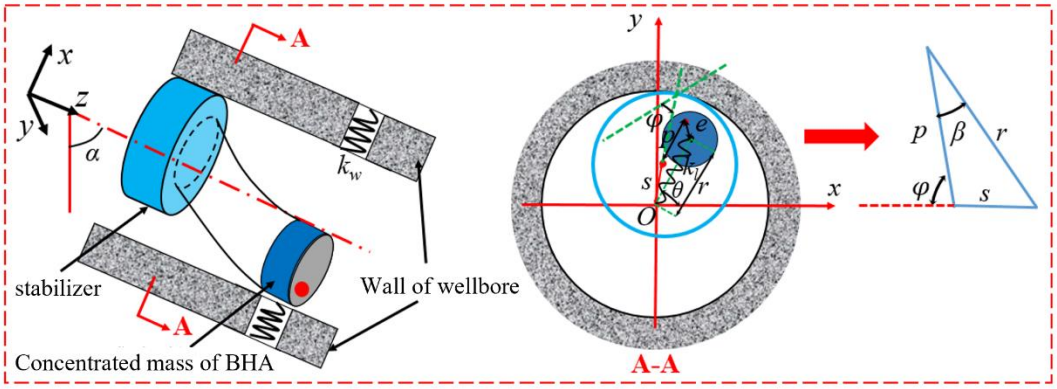

Fig. 2 The stabilizer-wellbore contact model

Based on the above analysis, the actual transverse bending deformations of the drill string and BHA below the neutral point can be determined by the root of the deformation compatibility conditions in the transverse direction [10]:

$$\begin{cases} \delta_{x1} = x_1 - \varepsilon_1 x_d - \varepsilon_2 x_s \\ \delta_{y_1} = y_1 - \varepsilon_1 y_d - \varepsilon_2 y_s \end{cases} \tag{5}$$

$$\begin{cases} \delta_{x2} = x_2 - \varepsilon_3 x_b - \varepsilon_4 x_s \\ \delta_{y_2} = y_2 - \varepsilon_3 y_b - \varepsilon_4 y_s \end{cases} \tag{6}$$

Where x_d and y_d, x_b and y_b represent the transverse displacements of the drill string and BHA, respectively, and their values are taken as zero. $\varepsilon_i = ld_i/l_1$ (i = 1, 2) and $\varepsilon_j = ld_j/l_2$ (j = 3, 4). l_1 and l_2 are the lengths of the drill string and BHA below the neutral point, respectively. When there is no contact between the stabilizer and the wellbore wall, the transverse displacements of the stabilizer are $x_s = x_2$ and $y_s = y_2$; when there is contact between the stabilizer and the wellbore wall, the transverse displacements of the stabilizer are $x_s = s \cdot cos\theta_2$ and $y_s = s \cdot sin\theta_2$, where θ_2 is the whirl angle of the BHA and s is the gap between the stabilizer and the wellbore wall.

Therefore, the actual bending strain potential energies V_3 and V_4 of the drill string and BHA below the neutral point, respectively, can be expressed as:

$$V_3 = \begin{cases} \frac{1}{2}k_{l1}\left(x_1 - \frac{ld_2}{l_1}x_2\right)^2 + \frac{1}{2}k_{l1}\left(y_1 - \frac{ld_2}{l_1}y_2\right)^2, x_2^2 + y_2^2 < s^2 \\ 0, x_2^2 + y_2^2 \geq s^2 \end{cases} \tag{7}$$

$$V_4 = \begin{cases} \frac{1}{2}k_{l2}\left(1 - ld_4/l_2\right)^2\left(x_2^2 + y_2^2\right), x_2^2 + y_2^2 < s^2 \\ 0, x_2^2 + y_2^2 \geq s^2 \end{cases} \tag{8}$$

Where kl_1 and kl_2 represent the equivalent transverse stiffness of the drill string and BHA below the neutral point, respectively.

In conclusion, the total potential energy V of the drill string vibration system is given by:

$$V = \sum_{i=1}^{4} V_i \tag{9}$$

Furthermore, during the energy absorption and release process, the total dissipated energy D of the drill string system is given by:

$$D = \frac{1}{2}c_{l1}\left(\dot{x}_1^2 + \dot{y}_1^2\right) + \frac{1}{2}c_{l2}\left(\dot{x}_2^2 + \dot{y}_2^2\right) + \frac{1}{2}c_t\left(\omega_t - \dot{\phi}_1\right)^2 + \frac{1}{2}c_{td}\left(\dot{\phi}_1 - \dot{\phi}_2\right)^2 + \frac{1}{2}c_z\left(\dot{z}_1 - \dot{z}_2\right)^2 \tag{10}$$

Where c_{l1} and c_{l2} are the transverse drag damping coefficients of the drilling fluid, c_{td} is the torsional damping coefficient of the drill string below the neutral point, c_z is the axial damping

ISSN: 1813-4890

coefficient of the drill string below the neutral point, and ω_t is the angular velocity of the top drive system.

By introducing the following Lagrangian equations, the differential equations of motion for the drill string vibration system can be established:

$$\frac{\partial}{\partial t}\left(\frac{\partial T}{\partial \dot{q}}\right)+\frac{\partial (V-T)}{\partial q}+\frac{\partial U}{\partial \dot{q}}=F \tag{11}$$

Where q is the generalized coordinate of the system, and the generalized coordinate set is [z_1, x_1, y_1, ϕ_1, z_2, x_2, y_2, ϕ_2]. $\dot{q}$ is the generalized velocity of the system, that is $\dot{q}=\frac{d\dot{q}}{dt}$. F is the generalized force of the system, and the generalized force set is [F_{z1}, F_{x1}, F_{y1}, $F_{\phi 1}$, F_{z2}, F_{x2}, F_{y2}, $F_{\phi 2}$].

By substituting equations (2), (9), and (10) into equation (11) and rearranging, the differential equations of motion for the drill string and BHA below the neutral point can be obtained:

(i) $x_2^2+y_2^2<s^2$

$$\begin{cases}
m_1\left(\ddot{x}_1-e_1\ddot{\phi}_1\sin\phi_1-e_1\dot{\phi}_1^2\cos\phi_1\right)+m_1 g\cos\alpha+k_{l1}\left(x_1-\frac{ld_2}{l_1}x_2\right)+c_{l1}\dot{x}_1=F_{x1}\\
m_1\left(\ddot{y}_1+e_1\ddot{\phi}_1\cos\phi_1-e_1\dot{\phi}_1^2\sin\phi_1\right)+k_{l1}\left(y_1-\frac{ld_2}{l_1}y_2\right)+c_{l1}\dot{y}_1=F_{y1}\\
m_1\ddot{z}_1-m_1 g\sin\alpha+k_z\left(z_1-z_2\right)+c_z\left(\dot{z}_1-\dot{z}_2\right)=F_{z1}\\
J_1\ddot{\phi}_1+m_1\left(e_1^2\ddot{\phi}_1-e_1\ddot{x}_1\sin\phi_1+e_1\ddot{y}_1\cos\phi_1\right)-m_1 g e_1\cos\alpha\cos\phi_1+k_{t1}\left(\phi_1-\phi_2\right)+k_t\left(\phi_1-\phi_t\right)\\
+c_t\left(\dot{\phi}_1-\omega_t\right)+c_{td}\left(\dot{\phi}_1-\dot{\phi}_2\right)=F_{\phi 1}\\
m_2\left(\ddot{x}_2-e_2\ddot{\phi}_2\sin\phi_2-e_2\dot{\phi}_2^2\cos\phi_2\right)+m_2 g\cos\alpha-\frac{ld_2}{l_1}k_{l1}\left(x_1-\frac{ld_2}{l_1}x_2\right)+k_{l2}\left(1-ld_4/l_2\right)^2 x_2+c_{l2}\dot{x}_2=F_{x2}\\
m_2\left(\ddot{y}_2+e_2\ddot{\phi}_2\cos\phi_2-e_2\dot{\phi}_2^2\sin\phi_2\right)-\frac{ld_2}{l_1}k_{l1}\left(y_1-\frac{ld_2}{l_1}y_2\right)+k_{l2}\left(1-ld_4/l_2\right)^2 y_2+c_{l2}\dot{y}_2=F_{y2}\\
m_2\ddot{z}_2-m_2 g\sin\alpha+k_z\left(z_2-z_1\right)+c_z\left(\dot{z}_2-\dot{z}_1\right)=F_{z2}\\
J_2\ddot{\phi}_2+m_2\left(e_2^2\ddot{\phi}_2-e_2\ddot{x}_2\sin\phi_2+e_2\ddot{y}_2\cos\phi_2\right)-m_2 g e_2\cos\alpha\cos\phi_2+k_{t1}\left(\phi_2-\phi_1\right)+c_{td}\left(\dot{\phi}_2-\dot{\phi}_1\right)=F_{\phi 2}
\end{cases} \tag{12}$$

(ii) $x_2^2+y_2^2\geq s^2$

$$\begin{cases}
m_1\left(\ddot{x}_1-e_1\ddot{\phi}_1\sin\phi_1-e_1\dot{\phi}_1^2\cos\phi_1\right)+m_1 g\cos\alpha+c_{l1}\dot{x}_1=F_{x1}\\
m_1\left(\ddot{y}_1+e_1\ddot{\phi}_1\cos\phi_1-e_1\dot{\phi}_1^2\sin\phi_1\right)+c_{l1}\dot{y}_1=F_{y1}\\
m_1\ddot{z}_1-m_1 g\sin\alpha+k_z\left(z_1-z_2\right)+c_z\left(\dot{z}_1-\dot{z}_2\right)=F_{z1}\\
J_1\ddot{\phi}_1+m_1\left(e_1^2\ddot{\phi}_1-e_1\ddot{x}_1\sin\phi_1+e_1\ddot{y}_1\cos\phi_1\right)-m_1 g e_1\cos\alpha\cos\phi_1+k_{t1}\left(\phi_1-\phi_2\right)+k_t\left(\phi_1-\phi_t\right)\\
+c_t\left(\dot{\phi}_1-\omega_t\right)+c_{td}\left(\dot{\phi}_1-\dot{\phi}_2\right)=F_{\phi 1}\\
m_2\left(\ddot{x}_2-e_2\ddot{\phi}_2\sin\phi_2-e_2\dot{\phi}_2^2\cos\phi_2\right)+m_2 g\cos\alpha+c_{l2}\dot{x}_2=F_{x2}\\
m_2\left(\ddot{y}_2+e_2\ddot{\phi}_2\cos\phi_2-e_2\dot{\phi}_2^2\sin\phi_2\right)+c_{l2}\dot{y}_2=F_{y2}\\
m_2\ddot{z}_2-m_2 g\sin\alpha+k_z\left(z_2-z_1\right)+c_z\left(\dot{z}_2-\dot{z}_1\right)=F_{z2}\\
J_2\ddot{\phi}_2+m_2\left(e_2^2\ddot{\phi}_2-e_2\ddot{x}_2\sin\phi_2+e_2\ddot{y}_2\cos\phi_2\right)-m_2 g e_2\cos\alpha\cos\phi_2+k_{t1}\left(\phi_2-\phi_1\right)+c_{td}\left(\dot{\phi}_2-\dot{\phi}_1\right)=F_{\phi 2}
\end{cases} \tag{13}$$

ISSN: 1813-4890

3. Dynamic analysis of the PZ5-2D drilling tool assembly: A case study

The motion differential equations of the drill string vibration system below the neutral point in the inclined wellbore have been derived, and the interaction between stabilizer and wellbore has been analyzed. Therefore, based on the second-order nonlinear differential equations shown in equations (12) and (13), the dynamic model of the drill string vibration system below the neutral point was established using the Matlab/Simulink module. The vibration characteristics of the drill string system were determined under different drilling pressures, top drive speeds, inclination angles, and bit types, and the influence of these parameters on the drill string dynamics was studied. By combining the actual drilling structural parameters of the PZ5-2D well in Pengzhou, the basic parameters of the system for numerical simulation were determined, as shown in Table 1.

Table 1 Basic system parameter

Parameter name	Value	unit	Parameter name	value	unit
Drill string eccentricity e	0.0127	m	Outside diameter of drill string D1	0.1016	m
Modulus of elasticity	210	GPa	Bore diameter of drill string d1	0.0932	m
Shear modulus	78	GPa	Bit radius R	0.1651	m
Acceleration of gravity	9.8	m/s2	Outside diameter of drill collar D2	0.1016	m
Inclination Angle α	60	°	Inside diameter of drill collar d2	0.0932	m
Gap value s2	0.0571	m	Friction coefficient u	0.35	/
Length of BHA l2	45	m	Coefficient of static friction ue	0.45	/
Bit coefficient nbit	1	/	Coefficient of dynamic friction ud	0.35	/
Parameter η	0.001	m	Steel density ρ	7850	kg/m3
Formation stiffness kf	4×106	N/m	Drilling fluid density ρf	1500	kg/m3
Wall stiffness kw	5×1011	N/m	Gap value s1	0.09625	m
Gap value s	0.02	m	Coefficient Ca	1.7	/
Coefficient Cd	1	/	Coefficient c	0.0378	Ns/rad
Top drive speed ωt	60(6.28)	r/min(rad/s)	WOB	40	kN

Based on the parameters shown in Tab. 1, the dynamic responses of the drill string and BHA below the neutral point were determined using Figs. 3 and 4. The initial conditions for the velocity and displacement of each degree of freedom of the drill string and BHA were set to zero. From Figs. 3(a) and 4(a), it can be observed that due to the effect of the gravity component of the inclined section, the lateral motion trajectory of the drill string and BHA below the neutral point is concentrated near the lower wellbore. Under the driving force of the top torque and the influence of wellbore friction, the drill string and BHA below the neutral point undergo reciprocating motion within a fan-shaped region along the bottom of the wellbore. Compared to the drill string, the BHA exhibits more intense lateral vibrations, as shown in Figs. 4(a-b). The BHA has a wider range of motion and larger lateral displacement fluctuations. Additionally, from the time-domain curves of the radial displacements of the drill string and BHA, it can be observed that collisions occur between the drill string/BHA and the wellbore. Under the effect

ISSN: 1813-4890

of nonlinear collision friction, the drill string and BHA undergo forward and reverse vortices, with more severe collisions resulting in greater fluctuations in the forward and reverse vortex velocities of the drill string, as shown in Figs. 3(d-e) and 4(d-e). The vortex velocity of the BHA fluctuates within the range of [-15, 10] rad/s, while the vortex velocity of the drill string fluctuates within the range of [-7, 5] rad/s. Figs. 3(f) and 4(f) demonstrate that for the torsional vibration of the drill string and BHA, the interaction between the drill bit and the formation leads to more severe torsional vibrations in the BHA. The rotational speed of the BHA exhibits continuous and significant fluctuations, reaching a relatively stable state after 7 seconds, with an average rotational speed close to the top drive speed. According to Figs. 3(c) and 4(c), it can be observed that the axial vibration of the drill string and BHA is closely related to their rotational speed. As the rotational speed increases, the axial vibration becomes more intense, and the BHA exhibits negative axial displacement, indicating a tendency for bit bouncing.

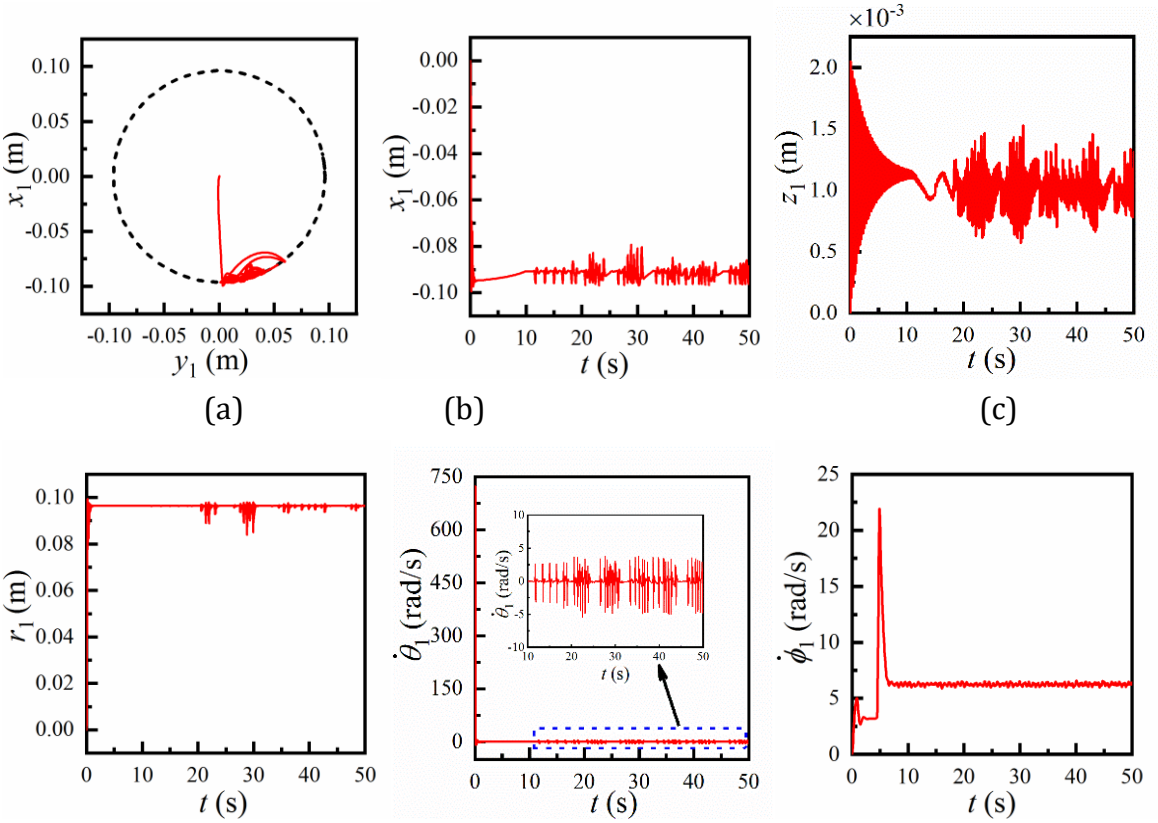

Fig.3 The dynamic response of the drill string below the neutral point

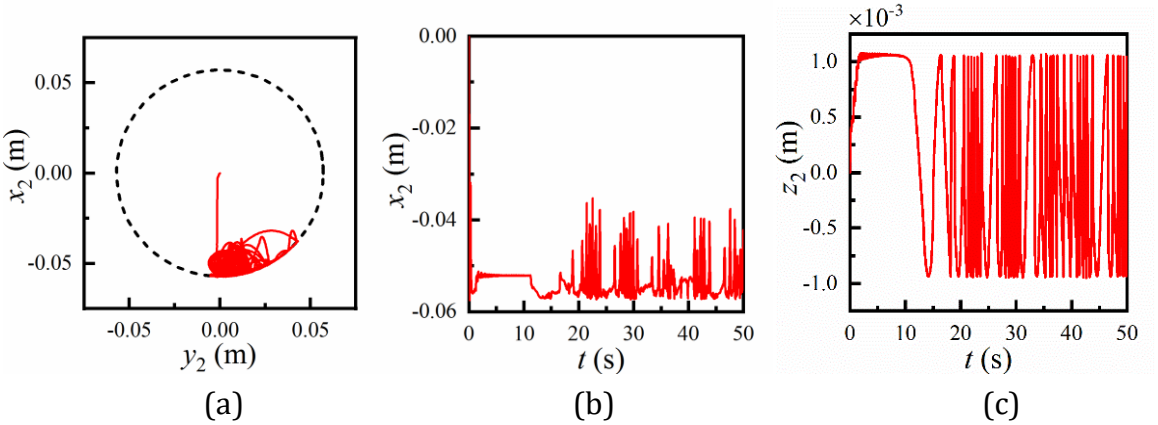

ISSN: 1813-4890

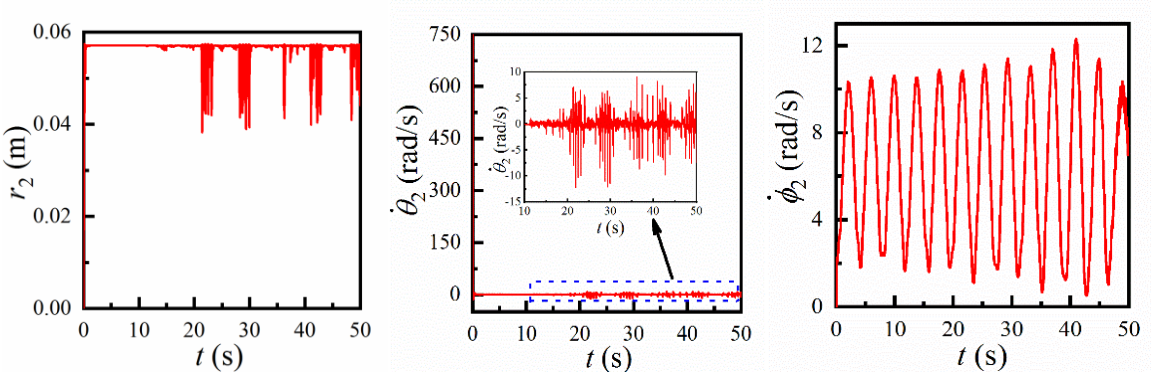

(d) (e) (f)

Fig. 4 The dynamic response of BHA

3.1 The effect of WOB.

In drilling engineering, the dynamic characteristics of the drill string and the rock-breaking efficiency of the drill bit are influenced by the drilling pressure. Therefore, under the conditions of a wellbore inclination angle of 60° and a top drive speed of 60 r/min, the dynamic behavior of the drill string and BHA below the neutral point was investigated with an increase in drilling pressure to 60 kN, 80 kN, and 100 kN. The numerical simulation results are shown in Figures 3-5 and 3-6, where the red, blue, and green curves correspond to the dynamic response of the drill string and BHA when the drilling pressures are 60 kN, 80 kN, and 100 kN, respectively. It can be clearly observed that the higher the applied drilling pressure, the smoother the response curve associated with lateral vibration of the drill string, as shown in Figs. 5(a-b) and 6(a-b). When the drilling pressure is 100 kN, the lateral motion trajectory of the drill string is relatively stable, and the lateral displacement along the x direction quickly converges to -0.09625 m, as shown in Fig. 5(c). As the drilling pressure increases, the number of collisions between the drill string and the wellbore decreases. As shown in Figs. 5(d) and 6(d), when the drilling pressure is 100 kN, the radial displacements of the drill string converge to 0.09625 m and 0.0571 m, respectively. This implies that the drill string and BHA are moving closely along the wellbore, while when the drilling pressure is 60 kN, the drill string and BHA experience multiple collisions with the wellbore. In addition, when there is no collision between the drill string and the wellbore, the phenomenon of positive and negative circulation disappears, and the circulation velocity almost approaches zero, as shown in Figs. 5(e) and 6(e). Furthermore, as the drilling pressure gradually increases, the axial vibration amplitude of the drill string decreases, as shown in Figs. 5(f) and 6(f). With time, the axial displacement of the drill string gradually converges to a smaller stable value. By combining Figs. 5(b) and 6(b), it can be observed that when the drill string and BHA undergo severe axial vibrations, the corresponding lateral displacement of the drill string also fluctuates dramatically, reflecting the coupled characteristics of axial and lateral motion of the drill string. However, as the drilling pressure increases, the rotation speed of the drill string fluctuates more severely, and there is a greater possibility of stick-slip motion, as shown in Figs. 5(c) and 6(c). When the drilling pressure is 100 kN, both the drill string and BHA experience stick-slip vibrations. Compared to the drill string, the BHA has a higher occurrence of stick-slip motion, as the interaction between the drill bit and formation hinders the rotation of the drill bit.

In summary, under conditions of higher drilling pressure, the drill string is prone to move closely along the wellbore, resulting in an increased frictional resistance torque on the drill string and leading to stick-slip motion. However, this helps to suppress axial and lateral vibrations, as well as positive and negative circulation, of the drill string and BHA.

ISSN: 1813-4890

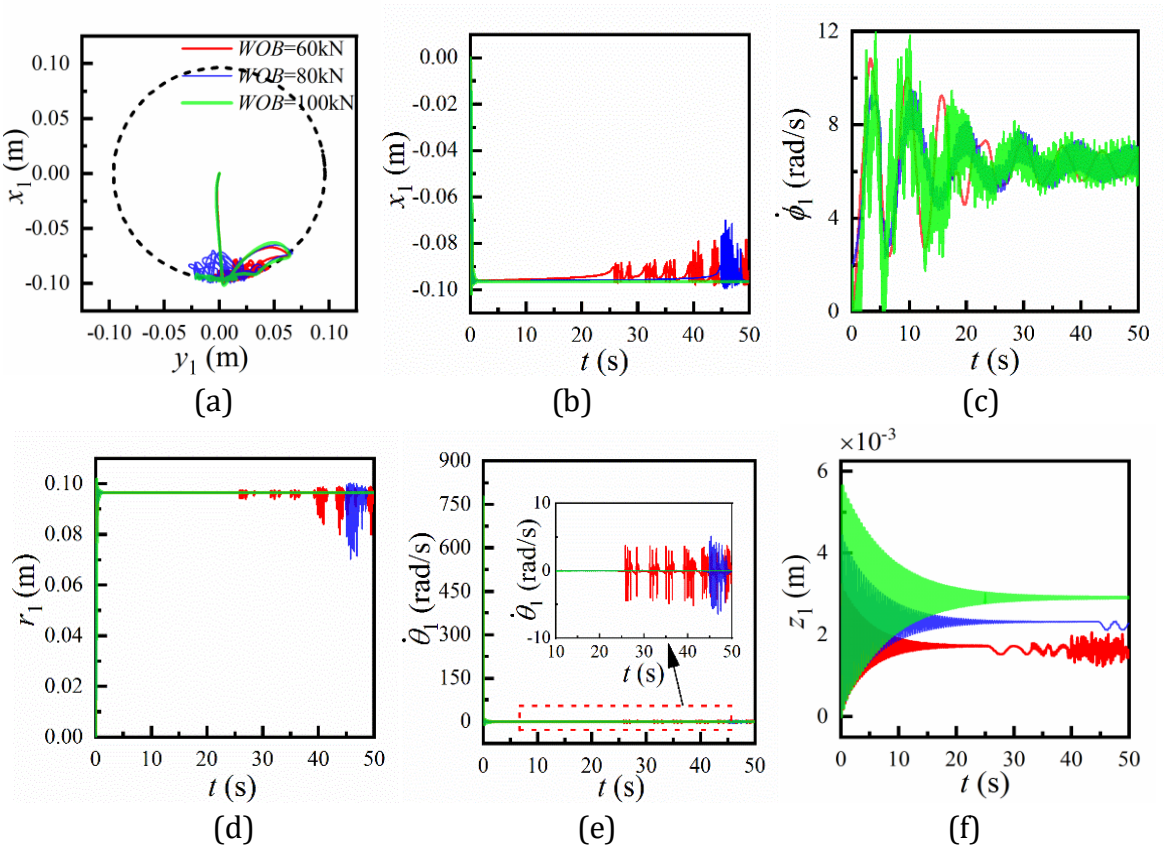

Fig. 5 Dynamic behavior of drill string with different WOB

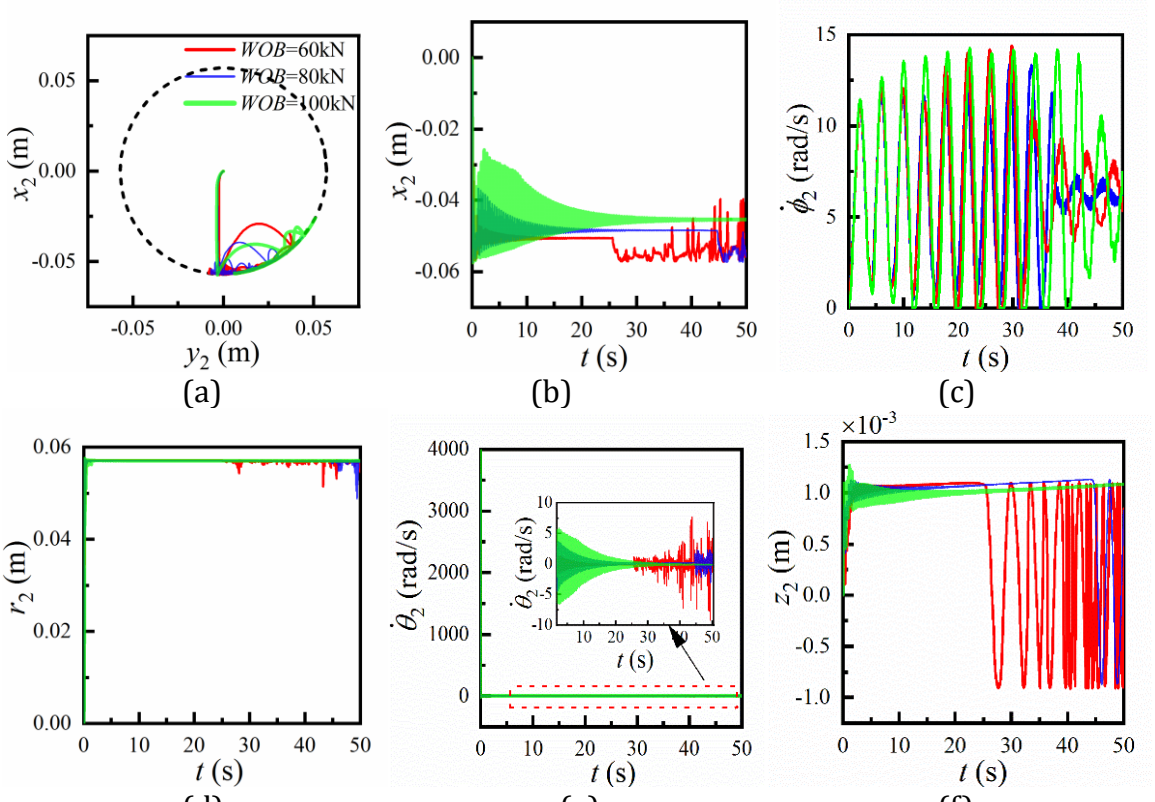

Fig. 6 Dynamic behavior of BHA with different WOB

ISSN: 1813-4890

4. Conclusion

(1) When drilling pressure exceeds a certain threshold, the drill string located below the neutral point may experience sideways bending, which increases frictional resistance on the system. This, in turn, can cause the drill string to exhibit stick-slip behavior. Nevertheless, if the drilling pressure is increased in an appropriate manner, it can help mitigate axial vibrations of the Bottom Hole Assembly (BHA).

(2) Changes in the top drive rotational speed can significantly impact the dynamic characteristics of the drill string system, particularly under the neutral point. Higher top drive rotational speeds result in increased drill string vibration. If the rotational speed is excessively high, the drill string may oscillate along the wellbore axis, which may lead to an increased incidence of wall sticking.

References

[1] PJ. Chen, DL. Gao, ZH. Wang, WJ. Huang, Study on aggressively working asing string in extended-reach well, J. Pet. Sci. Eng. 157 (2017) 604–616, http://dx.doi.org/10.1016/j.petrol.2017.07.059.

[2] J. Tian, Y. Yang, L. Yang, Vibration characteristics analysis and experimental study of horizontal drill string with wellbore random friction force, Arch. Appl.Mech. 87 (2017) 1439–1451.

[3] XB. Liu, N. Vlajic, XH. Long, G. Meng, B. Balakumar, Nonlinear motions of a flexible rotor with a drill bit: stick–slip and delay effect, Nonlinear Dynam. 72(1–2) (2013) 61–77, http:// dx.doi.org/ 10.1007/S11071-012-0690-x.

[4] ZQ. Huang, D. Xie, B. Xie, WL. Zhang, FX. Zhang, H. Lei, Investigation of PDC bit failure base on stick-slip vibration analysis of drilling string system plus drill bit, J. Sound Vib. 417 (2018) 97–109, http://dx.doi.org/10.1016/j.jsv.2017.11.053.

[5] S.Mohammadzadeh. Bina, H. Fujii, S. Tsuya, H. Kosukegawa, S. Naganawa, R.Harada, Evaluation of utilizing horizontal directional drilling technology for ground source heat pumps, Geothermics 85 (2020) 101769, http://dx.doi.org/10.1016/j.geothermics.2019.101769.

[6] EM. Navarro-Lopez, D. Cortes, Avoiding harmful oscillations in a drillstring through dynamical analysis, J. Sound Vib. 307 (2007) 152–171, http://dx.doi.org/10.1016/j.jsv.2007.06.037.

[7] M. Sarker, DG. Rideout, SD. Butt, Dynamic model for longitudinal and torsional motions of a horizontal oilwell drillstring with wellbore stick–slip friction, J. Pet. Sci. Eng. 150 (2017) 272–287, http://dx.doi.org/10.1016/j.petrol.2016.12.010.

[8] K. Nandakumar, M. Wiercigroch, Stability analysis of a state dependent delayed, coupled two DOF model of drill-string vibration, J. Sound Vib. 332 (2013) 2575–2592, http://dx.doi.org/ 10.1016/j.jsv.2012.12.020.

[9] Y. Briend, E. Chatelet, R. Dufour, M. Andrianoely, F. Legr, MS. Sousa, V. Steffen, S. Baudin, Dry-whip phenomenon in on-board rotordynamics: Modeling and experimentation, J. Sound Vib. 531 (2021) 116398, http://dx.doi.org/10.1016/j.jsv.2021.116398.

[10] L. Xiang, N. Gao, Coupled torsion-bending dynamic analysis of gear-rotor-bearing system with eccentricity fluctuation, Appl. Math. Model. 50 (2017) 569–584, http://dx.doi.org/ 10.1016/ j.apm.2017.06.026.